CHARGE MEASUREMENTS IN SwissFEL AND RESULTS OF AN ABSOLUTE CHARGE MEASUREMENT METHOD

G. L. Orlandi*, P. Craievich, M. M. Dehler, R. Ischebeck, F. Marcellini, D. Stäger
Paul Scherrer Institut, 5232 Villigen PSI, Switzerland

Abstract

A comparative measurement campaign of the beam charge was carried out at SwissFEL using the following instruments: Faraday-Cup (FC), Wall-Current-Monitor (WCM), Integrating-Current-Transformer (Bergoz Turbo-ICT-2) and the reference cavity of the Beam-Position-Monitor (BPM). The goal of the measurement campaign was to determine an absolute charge measurement method for a general purpose of instrument calibration and machine routine operation. Results of the absolute charge calibration method proposed for SwissFEL will be presented.

INTRODUCTION

In the electron linac driven SwissFEL – the X-ray laser facility of Paul Scherrer Institut (PSI, www.psi.ch) – two undulator lines can be simultaneously supplied at a maximum repetition rate of 100 Hz by electron bunches with a charge in the range 10-200 pC and energy of 6.2 GeV and 3.3 GeV, respectively. A 2-bunch train of charge is emitted by a photocathode with a time duration of a few ps for the single bunch and a time macro-structure of 28 ns, accelerated by a 3 GHz RF booster and 6 GHz RF linac and compressed up to a few fs by two magnetic chicanes. The two bunches are split apart by a RF kicker into a magnetic switchyard to be finally injected into the ARAMIS and ATHOS undulator lines [1, 2], respectively.

The measurement of the bunch charge at the different acceleration stages of a linac driven Free-Electron-Laser (FEL) is relevant for characterizing the beam features such as the tranverse emittance and peak current, for monitoring the correct transport of the beam through all the acceleration and compression stages, for protecting the machine from possible accidental beam losses and for a legal certification of the charge-per-hour accelerated by the machine.

In SwissFEL, the charge of each single bunch of the 28 ns long macro-structure can be measured at different position of the machine. Just downstream of the gun, a standard Bergoz ICT and a Bergoz Turbo-ICT-2 [3] can measure the integrated charge of the bunch train and the charge of the single bunch, respectively. At the gun, a Faraday-Cup (FC) and a Wall-Current-Monitor (WCM) are also available. The FC was initially installed just downstream of the SwissFEL gun to measure the dark current. The WCM is used in Swiss-FEL to measure the electron bunch charge and mainly to synchronize the photocathode laser and the radio frequency of the RF gun. In addition to the Turbo-ICT in the gun, three more Turbo-ICTs are available along the ARAMIS electron beam line as well as two Turbo-ICTs can provide

the charge readout at the beginning and at the end of the ATHOS electron beam line. A further monitor of the beam charge is represented by the cavity-BPM. The charge dependent signal of the monopole RF cavity of the BPM is used to normalize the dipole signal of the adjacent RF cavity which instead depends on the product of the charge and position of the bunch. The normalized dipole signal is hence processed to determine the bunch position in the horizontal and vertical directions. In SwissFEL, about two hundred cavity-BPMs are distributed all along the machine. The monopole RF signal of the cavity-BPMs has been so far calibrated against the charge readout of a reference Turbo-ICT-2 in order to provide an additional and a quite densely localized charge readout of the single bunch at 100 Hz.

The absolute calibration of the charge monitor is a crucial and sensitive issue in all the particle accelerators and, in that sense, SwissFEL does not makes an exception. The determination of an absolute method of charge calibration is even more stringent and necessary in linac facility where different charge monitors designed, realized and calibrated by distinct manufactures – quite often by a third party – are all together integrated in the machine as in the SwissFEL.

At the beginning of the SwissFEL project an agreement was signed between PSI and Bergoz for the realization of a fast Integrating-Current-Transformer (ICT) able to discriminate the 28 ns macro-structure of the SwissFEL beam in the charge range 10-200 pC. The company provided PSI with Turbo-ICT-2 sensors equipped with a factory calibration certification and a native front-end readout electronics. In order to perform a correct integration of the Turbo-ICT with the most general machine environment of the signal control and timing system of SwissFEL, the Turbo-ICT native electronics was interfaced with the standard back-end readout electronics in use at PSI.

Manufacturer company and PSI share a distinct role and action domain in the ICT set-up and operation. The company is responsible for the sensor calibration and front-end readout electronics while PSI is responsible for the back-end readout electronics and opeartions. Consequently, a clear recognition of the actions for bug-fixing and system improvements as well as every possible intervention of recalibration of a Turbo-ICT or correction of a charge readout discrepancy between different ICTs requires a complex formal procedure with possible local breaks of the machine operations as well as a large investment of beam time and manpower resources.

In order to ensure to PSI an absolute calibration procedure to be applied to all the charge monitors in operation at SwissFEL, the decision to develop in-house an independent charge measurement and calibration method was taken and realized as in the following described.

---

* gianluca.orlandi@psi.ch

THE SwissFEL CHARGE MONITORS

An overview of the charge monitor used in SwissFEL will be given in this section: Faraday-Cup (FC), Wall Current Monitor (WCM), cavity Beam Position Monitor (BPM). With the exception of the FC, all the other instruments are non destructive and can be used as online monitors during machine operations.

Integrating-Current-Transformer

In SwissFEL two type of Integrating Current Transformers (ICTs) produced by Bergoz [3] are in use: one standard ICT with BCM-IHR readout electronics and six Turbo-ICT-2s with BCM-RF electronics. The conventional ICT is installed just in front of the gun together with a Turbo-ICT-2. Three more Turbo-ICT-2s are installed all along the main branch of the ARAMIS linac; two Turbo-ICT-2s are installed in the linac of ATHOS.

In a standard ICT [3] the measurement of the beam charge results from the time integral of the beam induced current in the transformer. The proportionality between the time integral of the transformer current and the beam charge in a conventional ICT is ensured by the large spectral band of the frequency response from the near-DC (kHz) to the ten MHz regions [10, 11]. In SwissFEL, because of the large band of the frequency response and the relatively long integration time 5 µs [12], the dual bunch structure of the electron beam cannot be resolved by the standard ICT. Only the total charge with included the dark current contribution from the gun can be measured with a resolution ~pC.

The Turbo-ICT-2 produced by Bergoz for SwissFEL is instead able to discriminate the 28 ns time structure of the two bunches and to provide a measurement of the single bunch charge in the range 10-200 pC. The Turbo-ICT-2 is indeed equipped with a high frequency transformer ensuring a bandwidth up to several hundred MHz and with a narrow band-pass filter centered at around 180 MHz [3, 9, 13]. The output signal of the Turbo-ICT-2 is not a pulse but a resonance at the filter central frequency with an amplitude which is proportional to the bunch charge. The Turbo-ICT-2 output signal is practically insensitive to the dark current and, thanks to the short time length of the SwissFEL electron bunch, it is also insensitive to the electron bunch shape. The beam charge readout of the Turbo-ICT-2 is finally determined by the apex of the resonance that is measured by the sample-and-hold electronics of the BCM-RF. Charge resolution (rms) of the Turbo-ICT-2 is 0.1 pC (1%) within the range 10-200 pC. In order to meet the design constraint to discriminate the 28 ns spaced dual bunch structure, the native front-end filter amplifier has been modified by reducing the filter quality factor and hence decreasing the single bunch resonance duration [14].

Faraday-Cup

Based on the design of an analogous instrument already in use in the SLS linac, a Faraday-Cup (FC) is installed in SwissFEL in front of the 2.5 cell S-band gun of the 7 MeV photoinjector [4]. The FC sensor and the signal transmission line are designed as a 50 Ω coaxial structure with a bandwidth of more than 4 GHz, see Fig. 1. The FC can be inserted into the beam line by means of a pneumatic feedthrough. The FC was installed in SwissFEL to measure the dark current from the gun. Examples of FC waveforms acquired during machine operations at 200 pC are shown in Fig. 2.

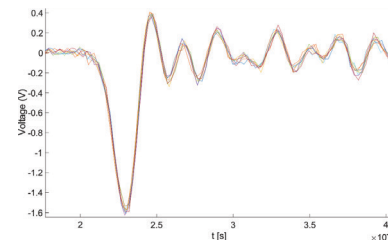Figure 1: Details of the SwissFEL FC sensor and transmission line.

Figure 2: FC waveforms acquired at SwissFEL during machine operations at 200 pC. A 30 dB attenuator was used to protect the oscilloscope during the measurements.

Wall-Current-Monitor

A Wall-Current-Monitor (WCM) is installed downstream of the SwissFEL gun. The signal induced by the electron beam on the WCM is used as a time reference for a coarse synchronization of the timing of the photocathode laser and the RF bucket in the gun. The time integration of the WCM output signal also allows the charge of the 2-bunch train structure to be determined.
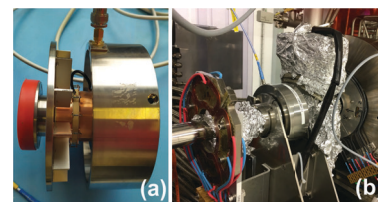

Figure 3: Images of the spare WCM (a) and SwissFEL WCM (b): nominal R_{gap} = 3.0±0.05 Ω (12 x 36 Ohm gap resistors) and NiZn ferrite ring.

A spare WCM – identical to the one installed in SwissFEL – is shown in the photo of Fig. 3. In the photo it is visible a set of 12 equally spaced 36 Ω resistors which bridge in parallel a gap in the beam pipe where a ceramic ring ensures the electrical insulation and the vacuum seal. A NiZn ferrite ring enclosed in the external metallic cylinder surrounds the
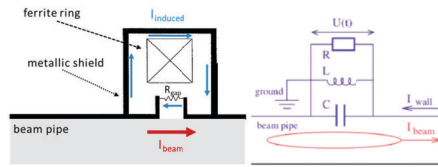
Figure 4: schematic sketch of the WCM and equivalent circuit model of the WCM as a parallel of an inductance L, gap resistor R and gap capacitor C.

resistor crown and the gap in the beam pipe, see Fig. 4. The external metallic cylinder constitutes a Faraday cage for the resistors. It also ensures a confinement of the electromagnetic field travelling with the electron beam as well as of the current induced into the metallic shielding by the fast time variation of the magnetic field trapped by the ferrite core [5]. The time integration of the voltage drop (V_{gap}) across the parallel of the resistors (R_{gap}) permits to determine the beam charge (Q):

$$Q = \frac{1}{R_{gap}} \int_{t_0}^{t_1} V_{gap}(t)\, dt \;. \tag{1}$$

Typical time windowing of the WCM signal readout at Swiss-FEL is in the order of ten nanoseconds. With reference to the equivalent circuit model in Fig. 4 it is possible to estimate the bandwidth of the WCM response in the frequency domain as well as to better understand the limitation of this instrument in determining a precise measurement of the beam charge. The inductance L represented by the ferrite and the metallic shield affects the low frequency response of the WCM with a cutoff frequency f_{low} that prevents to measure the DC component of the current input signal of the WCM:

$$f_{low} = \frac{R_{gap}}{2\pi L}. \tag{2}$$

The gap in the vacuum pipe filled with the ceramic ring acts as a capacitor (C) which is responsible for a high frequency cutoff of the WCM frequency response (tipically in the GHz region):

$$f_{high} = \frac{1}{2\pi R_{gap} C}. \tag{3}$$

A correct determination of the gap resistance R_{gap} is crucial for a precise measurement of the absolute charge from the WCM. The SwissFEL WCM was the result of an adaptation to the specific case of a former instrument already developed for SLS [4]. With respect to the former SLS model, the resistance of the resistor parallel in the SwissFEL WCM was increased from the nominal value of $1\,\Omega$ to $3\,\Omega$ to improve the sensitivity.

Both the WCM installed in SwissFEL and the spare WCM prototype have been experimentally characterized. The achieved experimental results have been compared with results of numerical simulations of a model of the SwissFEL WCM developed by means of the codes *CST Studio Suite* [6] and *ANSYS HFSS* [7]. Details on the work of experimental characterization and numerical modelling of the WCM will be presented in a dedicated article [8]. In the present paper, the main results and conclusions will be summarized.

Gap resistance and inductance of both the SwissFEL and the spare WCM were determined by measuring the reflection coefficient S_{11} at the WCM output port by means of a Vector Network Analyzer (VNA). For the spare WCM, the measurement results of the reflection coefficient S_{11} confirmed the expected nominal value of the gap resistance ($R_{gap} = 3\,\Omega$) and permitted to determine the inductance driven low frequency cutoff of the WCM bandwidth $f_{low} \simeq 200\,\text{kHz}$. A gap resistance ($R_{gap} = 3.55\,\Omega$) larger than the nominal value $3.0\,\Omega$ was instead measured in the SwissFEL WCM. Since the SwissFEL WCM cannot be inspected, possible explanation of this mismatch is the accidental failure or damage of 2 of the 12 resistors bridging the ceramic gap.

A deeper insight into the question of the gap resistance of the SwissFEL WCM and of the value of the gap resistance to be used for the charge calculation in Eq. (1) was obtained thanks to a complete characterization with a VNA of the transfer function of the spare WCM prototype and a comparison with the numerical predictions from the CST model of the WCM.

For the VNA measurement of the transfer function of the spare WCM

$$Z(\omega) = \frac{V_{out}(\omega)}{I_{beam}(\omega)} [\Omega] \tag{4}$$

a dedicated testing workbench based on the coaxial wire method was set up in the laboratory, see Fig. 5. According

Figure 5: Laboratory setup for the measurement with a VNA of the WCM transfer function by means of the coaxial wire method.

to the VNA measurements, the transfer function shows the expected low frequency cutoff and a constant value in the frequency region up to several MHz where it is possible to evaluate the value of the impedance $Z(\omega) \simeq R_{gap}$ to be used for the charge calculation in Eq. (1). The estimated value of the gap impedance underestimates of about $5 - 6\%$ the expected nominal value of $2.83\,\Omega$ resulting from the parallel of the $3.0\,\Omega$ of the resistor crown across the gap and the $50\,\Omega$ load of the VNA [8].

In order to better investigate the discrepancy observed in the spare WCM between the low frequency measurement of the transfer impedance and the expected nominal value of the gap resitance, CST numerical simulations were performed. Numerical simulation from CST of the voltage signal across the resistor parallel and the related frequency spectrum for a Gaussian electron bunch with a rms pulse width of $\sigma = 25\,\text{ps}$ are shown in Fig. 6. The size of the 3D mesh defining the CST computing grid as well as the electron bunch length of $25\,\text{ps}$ – corresponding to a sampling frequency up to 13 GHz

– were optimized in order to ensure the required asymptotic convergence of the numerical predictions in a reasonable and affordable computing time. As shown in Fig. 6, the CST frequency spectrum of the WCM voltage is characterized by the expected constant amplitude in a frequency region from the near-DC up to a few hundreds MHz. In correspondence of this frequency region the time integration of the WCM output signal via Eq. (1) can be performed with respect to a well defined value of the gap resistance. At higher frequencies, the spectral distribution of the WCM voltage also shows a broadband peak around 1.5 GHz and a sharp peak at about 4.7 GHz. The origin of the 1.5 GHz broad band peak in the frequency spectrum of the WCM output voltage – Fig. 6(b) – can be explained [5] as the result of the mismatch of the gap resistance with the impedance of a parallel transmission line represented by the ceramic gap. CST numerical simulations of the frequency spectrum of the WCM voltage as a function of the gap resistance confirmed such hypothesis [8]. About the origin of the 4.7 GHz sharp peak in the voltage frequency spectrum, which is responsible of the fast oscillation characterizing the quenching tail of the voltage signal in Fig. 6(a), this is due to a spurious resonance occurring in the WCM beam pipe. Such a resonance is caused by the step transition from the outer beam pipe into the inner part of the WCM as demonstrated in [8] by means of an eigenmode simulation of the WCM performed with the code *ANSYS HFSS*.

About the aforementioned discrepancy of the nominal value of the gap resistance of the spare WCM with respect to the result of the VNA characterization, numerical simulations with the CST code allowed us to better understand the origin of this mismatch. It was indeed observed [8] that the outcome of the time integration of the WCM gap voltage in CST via Eq. (1) depends on the model assumed for the permeability μ of the NiZn ferrite. According to an ideal model of the ferrite with a constant value of the permeability $\mu = const$ in the considered integration frequency band, the result of the time integration of the gap voltage fits with the 200 pC input charge of the CST simulation. Conversely, if a more realistic and frequency dependent model for the ferrite permeability $\mu(\omega) = \mu'(\omega) - i\mu''(\omega)$ is implemented in CST, the time integration of the resulting gap voltage underestimates the input value of the beam charge. Explanation of this behaviour is the presence of ohmic losses inside the ferrite core due to the imaginary part of the complex expression of the ferrite inductance L when a dispersive model for the permeability μ is considered. According to a more realistic dispersive model of the ferrite, in the circuital model of the WCM sketched in Fig. 4, an additional ohmic resistance $R_L(\omega)$ should be added in series with the inductance L(ω). The presence of ohmic losses in the ferrite can explain hence the observed mismatch of the gap resistance measured during the transfer function characterization of the spare WCM with respect to the expected nominal value.

In conclusion, on the basis of the experimental results of the transfer impedance measurements of the spare WCM we can estimate that the gap impedance is 5–6% less than

the expected nominal value 2.83 Ω (parallel of 3.0 Ω and 50 Ω) because of the ohmic losses from the ferrite. Since it is practically impossible to repeat the same measurement of the transfer impedance in the SwissFEL WCM, we assume that the same estimate of the ohmic losses of the spare WCM ferrite can be also applied to the SwissFEL WCM since the two WCMs are in principle identical. On the basis of this assumption on the ohmic losses of the SwissFEL WCM, the low-frequency value of the transfer impedance $Z_L(\omega)$ to be used in Eq. (1) instead of the nominal gap resistance R_{gap} = 3.31 Ω (parallel of 3.55 and 50 Ω) should be $Z_{L,exp}(\omega)$ = 3.11 Ω. CST numerical simulations of the WCM transfer impedance based on the best up to date available dispersion model of the ferrite situate the value of the transfer impedance at $Z_{L,theo}(\omega)$ = 3.26 Ω. Finally, to the best of our up to date experimental and theoretical knowledge of the SwissFEL WCM we can estimate a low-frequency transfer impedance of $Z_L(\omega) = 3.11 - 3.26$ Ω (parallel with 50 Ω already included).

In Fig. 7, the measured output waveform of the SwissFEL WCM (upper plot) as well as the time integration of the output signal via Eq. (1) as a function of the integration time (lower plot) are shown for a nominal charge of the single bunch of 200 pC (Bunch-2, when Bunch-1 is OFF). In the plot of the time integral of the WCM waveform, the negative slope before time=0 is due to the integration of a background (most likely a RF environment background coming from the gun); the negative slope after time=0 is instead due to the combined effect of the background and of the absence of the DC component in the frequency distribution of the signal acquired by the WCM. The determination of the beam charge from the plot of the time integration of the waveform – Fig. 7 lower plot – can be performed by applying a suitable fitting procedure to the curve slopes around time=0 as more diffusely described in [8].
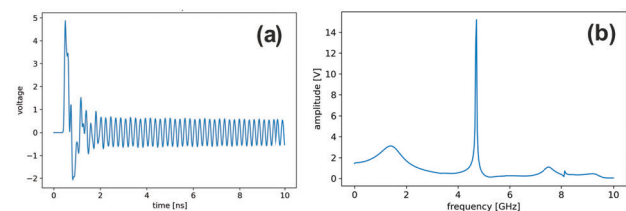

Figure 6: CST numerical simulation of the WCM output signal for an electron bunch length of 25 ps in the time domain (a) and in the related frequency domain (b).

Cavity-Beam-Position-Monitor and Method for Measuring the Beam Charge

The method for determining the beam charge from the analysis of the charge excited monopole signal in the cavity BPM has been proposed and implemented at SwissFEL by one of the authors (F.M.).

About 200 cavity BPMs are distributed along the Swiss-FEL linacs, transfer and undulator lines. They consists of
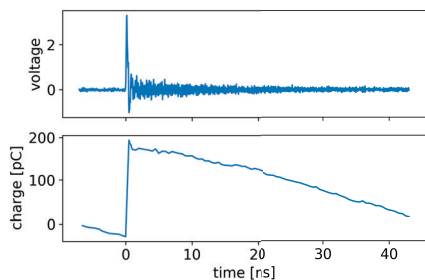
Figure 7: SwissFEL WCM signal readout of the single bunch with nominal charge 200 pC: (upper plot) measured output waveform; (lower plot) time integration of the WCM waveform via Eq. (1) as a function of the integration time.

two cavities: a so called position cavity resonating at the TM_{110} mode (dipole) and a reference cavity designed to resonate at the TM_{010} mode (monopole) [17]. Cavity BPMs ensure at SwissFEL the tracking of the beam orbit of the 2-bunch beam structure in the horizontal and vertical direction and the monitoring of the single bunch charge. The BPM sensitivity largely covers the 10-200 pC range ensuring a beam centroid positioning with a spatial resolution up to the sub-micrometer scale. More details on the cavity BPM performance and application as position monitor in [15, 16]. In the present context, our attention will be focused on the BPMs as charge monitors. During normal machine operation at SwissFEL, the monopole cavity signal of the BPMs provides a shot-to-shot estimate of the beam charge to the users. For normal machine operations, the calibration of the BPM monopole signal is performed against a reference Turbo-ICT-2: i.e., the BPM monopole ADC signal – as processed by the front-end electronics – is converted into a charge dimensional signal thanks to the comparison with the absolute charge readout of a reference Turbo-ICT-2. It should be noted that, in the application of the method of the cavity BPM for absolute charge measurements as below described, the monopole signal is directly acquired by an external oscilloscope and not from the standard BPM ADC.

Depending on the beam pipe aperture, four different types of cavity BPM are installed in SwissFEL. Furthermore, they can be classified in two types according to the working frequency: 3.284 GHz and low quality factor and 4.926 GHz and high quality factor. Each BPM is a double cavity device, where one cavity (usually called reference cavity) is used to normalize the signal detected by the other cavity to the beam charge. The output of the reference cavity comes from the energy that the beam releases on the TM_{010} cavity mode, and, since its sensitivity to beam position is negligible, it depends on the beam charge only. For our estimate of the SwissFEL bunch charges, we measured the output signal of several BPMs along the machine. The measurements setup simply consisted of a 16 GHz, 40 GS/s oscilloscope, connected to the cable that brings the BPM reference cavity signal to the technical gallery and a low pass filter, with cut-off frequency between the TM_{010} mode and the first HOM

frequencies, to isolate the contribution of the TM_{010} mode to the measured waveform. A number of waveforms have been grabbed for each BPM, at the bunch repetition rate (see Fig. 8). From the theory the signal $V_{out}(t)$ at the cavity output is:

$$V_{out}(t) = \quad q\omega\sqrt{\frac{Z}{Q_e}}R/Qe^{-\frac{\omega t}{2Q_L}}\cos(\omega t), \qquad (5)$$

where q is the bunch charge; ω is the angular frequency of the cavity TM_{010} mode; Z is the characteristic impedance of the cavity output line (50 Ohms in our case); R/Q is a RF parameter depending on the cavity geometry; $Q_e = \omega U/P_{out}$ is the cavity external quality factor (U is the cavity stored energy and P_{out} the power coupled out of the cavity); $Q_L = \omega U/(P_{wall} + P_{out})$ is the cavity loaded quality factor, which takes into account also the power lost P_{wall} in the cavity walls.

Every single BPM has been measured to determine its individual values of ω, Q_L and Q_e. There are also quite complicate techniques to measure R/Q, but we believe that numerical simulations can estimate its value even with larger precision. So, we assumed that all the BPMs of the same type have the same R/Q, and this was obtained by simulations with two different codes (HFSS and CST). Therefore, the bunch charge can be measured fitting the oscilloscope waveforms with the formula in Eq. (5), where the only free parameter is q. The attenuation of all the cables used in the measurements has also been measured and the amplitude of $V_{out}(t)$ scaled accordingly. The low-pass filter employed in the measurement has also been considered in the final expression used in the fit (see Fig. 9).
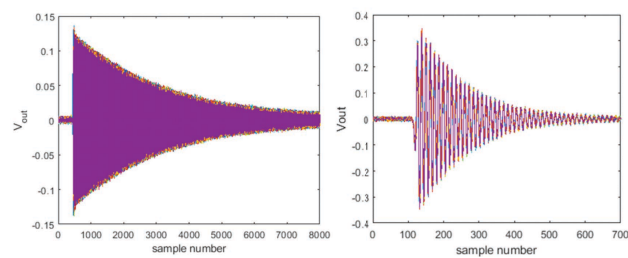

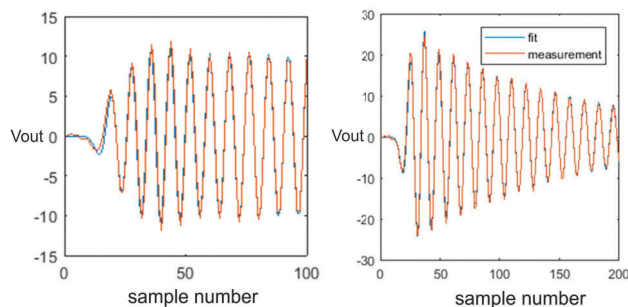Figure 8: Waveforms measured with the oscilloscope for one high Q (left) and one low Q (right) BPM.

Figure 9: Examples of fittings for a high Q (left) and one low Q (right) BPM.

ABSOLUTE CHARGE MEASUREMENTS AT SwissFEL

The Method

In the last couple of years several sessions of beam charge measurements were carried out at SwissFEL. Goal of this campaign of measurements was the definition of an univocal method for the absolute calibration of the non-descructive charge monitors of SwissFEL.

As mentioned above, the procedure so far adopted for calibrating the amplitude of the reference cavity signal of the BPMs involves using the reading of a reference Turbo-ICT-2 in the linac. As it is evident from the plot in Fig. 10 (red lines), the Turbo-ICT-2 readings along the linac are not constant and the choice of the reference Turbo-ICT-2 for the calibration is made in an arbitrary way. The question that raised a few years ago was whether it was possible to make absolute charge measurements using signals from the BPM reference cavities. In addition, to validate the charge measurements from the BPM, before using them as a comparison and subsequent calibration of the ICT, the charge values obtained from the cavity BPMs were compared with the readings from the WCM and the FC.

For such a purpose, the WCM of SwissFEL was the object of a careful work of experimental characterization and numerical modelling as described in previous section. About the cavity BPMs, all the knowledge of the characterization parameters was already available since they have been designed and experimentally characterized at PSI. Furthermore, the attenuation of the RF cables used for the cavity BPMs was also very precisely measured exactly at the frequency of resonance of the cavity. Charge measurements with FC were also performed. With respect to cavity BPM results we observed the FC underestimates of about 7% the beam charge.

In conclusion, behind the work carried out in the last couple of years on the subject of the charge measurements at SwissFEL, there were the following objectives: (1) check the reliability of the WCM and cavity BPM as absolute charge calibration tools; (2) on the basis of the charge calibration reference established by means of the WCM and cavity BPMs, proceed with the alignment of all the charge monitor in operation at SwissFEL in order to verify the long term stability and the possible time drift of the intrinsic calibration of each system. In the following paragraph, the results obtained in the definition of an absolute calibration method for the charge monitors of SwissFEL will be presented.

The Results

Results of the measurements of beam charge carried out in SwissFEL by acquiring the signal from the monopole RF cavity of several BPMs all along the machine are shown in Figs. 10. The BPM charge measurements of the electron beam charge plotted in Figs. 10 were obtained by applying the analysis method of the cavity BPM monopole signal as described in a dedicated paragraph. The cavity BPM results of the beam charge for bunch-1 and bunch-2 are compared
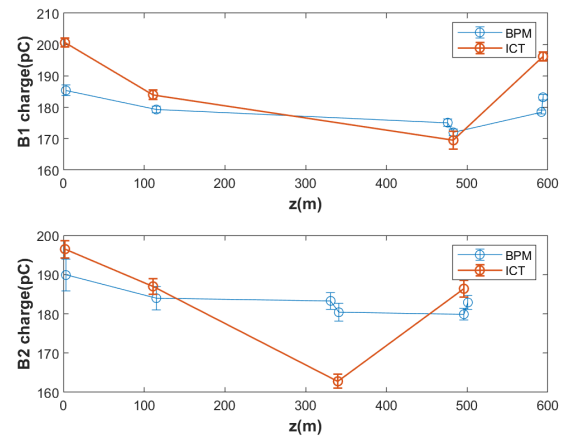

Figure 10: Comparison of charge measurements from Turbo-ICT-2 and cavity BPM all along the ARAMIS and ATHOS electron beam lines: bunch-1 (B1) (upper plot); bunch-2 (B2) (lower plot).

in Figs. 10 with analogous measurement results from the closest Turbo-ICT-2s. The acquisition of the measured data shown in Figs. 10 was not simultaneous but carried out individually for single device over a time interval of several hours. The corresponding Turbo-ICT-2s measurements were not synchronous but simultaneous to the cavity BPM measurements. The analysis of the data reported in Figs. 10 for bunch-1 (same considerations apply to the bunch-2 case) shows a relative systematic offset of the Turbo-ICT-2s along the machine and a substantial alignment of the cavity BPM measurements within the statistical error bars. Furthermore, it can be observed that some of the Turbo-ICT-2s provide a charge readout very close to the cavity BPM results. With respect to the charge measurements of the first Turbo-ICT, the average of the cavity BPM measurements in Fig. 10 is about 20 pC smaller: with respect to the bunch-1 charge readout of the first Turbo-ICT-2, the mean value of the charge measured by the cavity BPM is indeed 10% ± 2% smaller. In a further dedicated measurement session carried out in the high energy part of ARAMIS, a similar percentage offset of 10% ± 3% was observed in the mean value of the cavity BPM charge readouts for bunch-1 with respect to the first Turbo-ICT-2 (which is our reference ICT in this comparison). It should be noted that the dispersion affecting the measurements results of the different cavity BPMs in Fig. 10 may have a statistical and systematic origin. A statistical dispersion of the cavity BPM data can be expected since the measurement acquisition is not simultaneous (several hours needed for the acquisition of the complete set of measurements) and passing from a device to the other fluctuation of the beam charge can occur. The possible systematic error in the cavity BPM measurements can be instead explained by the incertitude in the attenuation measured for each RF cable.

In addition to the Turbo-ICT-2 and cavity BPM measurements carried out for bunch-1 and bunch-2 at a constant charge of 200 pC all along the ARAMIS and ATHOS elec-
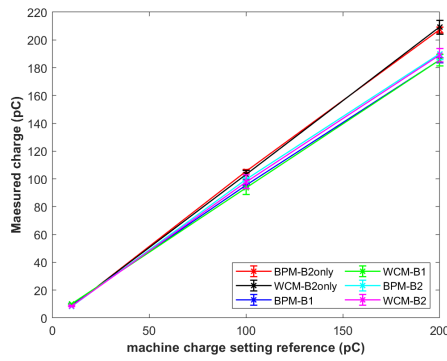
Figure 11: Comparison of the charge readout from the WCM and cavity BPM charge readout vs machine setting charge. The WCM and the cavity BPM are placed at coordinate z=0.58 m and z=3.01 m from the gun cathode, respectively.

tron beam line, simultaneous measurements were performed for a variable beam charge (10, 100 and 200 pC) by means of the first Turbo-ICT-2 placed at a distance of z=1.86 m from the gun cathode, the first cavity BPM placed at z=3.0 m and the WCM placed at z=0.58 m for three different acquisition settings, see Fig. 11: measurement of bunch-2 only (no bunch-1 emitted by the gun); measurement of bunch-1 in presence of bunch-2; measurement of bunch-2 in presence of bunch-1. Under the hypothesis of a transfer impedance $Z_L(\omega) = 3.26\,\Omega$ for the SwissFEL WCM the ratio of the WCM readout over the cavity BPM readouts for the different charge values are reported in Table 1. Taking into account the incertitude on the value of the transfer impedance of the WCM as above described ($Z_L(\omega) = 3.11 - 3.26\,\Omega$), we can very optimistically guess that the reliability of the WCM compared to the cavity BPM is within ±5%. Moreover, with respect to the bunch-1 charge readout of the first Turbo-ICT-2 at 200 pC – see Fig. 11 – the charge readout of the first cavity BPM at the gun is about $(8 \pm 1)\%$ smaller.

In conclusion, on the basis of the comparative study of the experimental results of the charge measurements for bunch-1 from the first Turbo-ICT-2 at the gun and from the cavity BPMs at the gun and all along the machine, the criterion that we can assume in a procedure of alignment of all the charge monitors in SwissFEL under the hypothesis of full transmission of the machine is the following: for a charge readout of 200 pC of the very first Turbo-ICT-2, the correct alignment value of all the charge monitors in SwissFEL – included the first Turbo-ICT-2 – should be about $(9 \pm 2\%)$ less, i.e., the aggregate outcome from the correction factors so far obtained ($10\% \pm 2\%$, $10\% \pm 3\%$, $8 \pm 1\%$).

Presently, the evaluation of the aforementioned charge alignment factor of the charge monitor in SwissFEL is only based on the absolute charge measurements of the cavity BPM which cannot be corroborate by the WCM which is affected by an incertitude that can be optimistically estimated in ±5%. Further numerical studies and experimental characterization will be needed to better characterize the SwissFEL WCM; the present impossibility to remove it from the beam line makes this goal quite hard to achieve. Further cavity BPM measurements in a simultaneous acquisition with the Turbo-ICT-2s are necessary to better quantify the aforementioned percentage calibration factor of the charge readout of the SwissFEL charge monitors as well.

Table 1 shows the ratio of the WCM over cavity BPM charge readout measured in SwissFEL for different acquisition settings and for different nominal values of the charge 10, 100 and 200 pC (see Fig. 11). Measurement of bunch-2 only (no bunch-1 emitted by the gun), measurement of bunch-1 in presence of bunch-2, and measurement of bunch-2 in presence of bunch-1. In the WCM calculation of the charge by means of Eq. (1) an impedance of $Z_t = 3.26\,\Omega$ (parallel of the estimated transfer impedance with the $50\,\Omega$ load of the scope) was assumed in agreement with the results of the CST characterization of the SwissFEL WCM (see related paragraph).

Table 1: Ratio of the WCM over Cavity BPM Charge Readout Measured in SwissFEL for Different Charge Values

Nominal charge	200 pC	100 pC	10 pC
WCM/BPM bunch-2 only	1.0092	0.9773	1.0361
WCM/BPM bunch-1	1.0011	0.9770	1.0204
WCM/BPM bunch-2	0.9953	0.9819	1.0341

CONCLUSIONS AND OUTLOOK

In the present paper a review of the charge monitors in operation at SwissFEL is presented. Results of a recent characterization of the SwissFEL WCM based on experimental measurements and code aided modelling are also presented. The numerical and experimental characterization of the SwissFEL WCM did not dissolve an incertitude in the WCM calibration parameters that we optimistically estimate in ±5%. A new method for determining the beam charge from the monopole RF signal of the cavity BPM is presented as well as the experimental results of its practical implementation at SwissFEL. Cavity BPMs showed a more robust and statistically consistent reliability in the measurement of the beam charge in SwissFEL. They demonstrated to be an useful tool to determine an absolute measurement of the beam charge in SwissFEL.

ACKNOWLEDGEMENTS

REFERENCES

[1] E. Prat *et al.*, "A compact and cost-effective hard X-ray free-electron laser driven by a high-brightness and low-energy

electron beam", *Nature Photonics*, vol. 14, pp. 748–754, 2020. `doi:10.1038/s41566-020-00712-8`

[2] R. Ganter *et al.*, "The SwissFEL soft X-ray free-electron laser beamline: Athos", *J. Synchrotron Rad.*, vol. 26, pp. 1073–1084, 2019. `doi:10.1107/S1600577519003928`

[3] Bergoz Instrumentation, *Integrating Current Transformer and Beam Charge Monitor*. `https://www.bergoz.com/en/ict-bcm-ihr`

[4] M. Dach, M. Dehler, A. Jaggi, P. Kramert, M. Pedrozzi, V. Schlott, and A. Streun, "SLS linac diagnostics-commissioning results", *AIP Conference Proceedings*, vol. 546, p. 563, 2000. `doi:10.1063/1.1342631`

[5] R. Webber, "Longitudinal emittance: An introduction to the concept and survey of measurement techniques including design of a wall current monitor", *AIP Conference Proceedings*, vol. 212, p. 85, 1990. `doi:10.1063/1.39712`

[6] *CST Studio Suite*, Dassault Systemes. `https://www.3ds.com/products-services/simulia/products/cst-studio-suite/`

[7] *ANSYS HFSS*, `https://www.ansys.com/products/electronics/ansys-hfss`

[8] D. Stäger *et al.*, "Characterization of the SwissFEL Wall Current Monitor: experimental and numerical simulation results", to be submitted for publication.

[9] S. Artinian, J. F. Bergoz, F. Stulle, P. Pollet, and V. Schlott, "Development and First Tests of a High Sensitivity Charge Monitor for SwissFEL", in *Proc. IBIC'12*, Tsukuba, Japan, Oct. 2012, paper MOPB87, pp. 287–290. `https://jacow.org/IBIC2012/papers/mopb87.pdf`

[10] K. Nakamura, D. E. Mittelberger, A. J. Gonsalves, J. Daniels, H.-S. Mao, F. Stulle, J. Bergoz, and W. P. Leemans, "Picocoulomb charge measured at BELLA to percent-level precision using a Turbo-ICT", *Plasma Phys. Control. Fusion*, vol. 58, p. 034010, 2016. `doi:10.1088/0741-3335/58/3/034010`

[11] F. Stulle, J. Bergoz, W.P. Leemans, and K. Nakamura, "Single Pulse Sub-Picocoulomb Charge Measured by a Turbo-ICT in a Laser Plasma Accelerator", in *Proc. IBIC'16*, Barcelona, Spain, Sep. 2016, pp. 119–122. `doi:10.18429/JACoW-IBIC2016-MOPG35`

[12] R. Ischebeck *et al.*, "Overview of Beam Instrumentation Activities for SwissFEL", in *Proc. IBIC'14*, Monterey, CA, USA, paper MOPF31, pp. 119–123, 2014. `https://jacow.org/IBIC2014/papers/mopf31.pdf`

[13] F. Stulle and J.F. Bergoz, "Turbo-ICT Pico-Coulomb Calibration to Percent-level Accuracy", in *Proc. FEL'15*, Daejeon, Korea, pp. 118–121, 2015. `doi:10.18429/JACoW-FEL2015-MOP041`

[14] S. Artinian, J. Bergoz, F. Stulle, P. Pollet, and V. Schlott, "Goubau Line and Beam Characterization of TURBO-ICT for SwissFEL", in *Proc. IPAC'13*, Shanghai, China, p. 476, paper MOPME005, 2013. `https://jacow.org/ipac2013/papers/mopme005.pdf`

[15] B. Keil, R. Baldinger, R. Ditter, W. Koprek, R. Kramert, G. Marinkovic, M. Roggli, M. Stadler, and D. M. Treyer, "A Generic BPM Electronics Platform for European XFEL, SwissFEL and SLS", in *Proc. IBIC'12*, Tsukuba, Japan, Oct. 2012, paper MOCB02, pp. 11–15. `https://jacow.org/IBIC2012/papers/MOCB02.pdf`

[16] T. Schietinger *et al.*, "Commissioning experience and beam physics measurements at the SwissFEL Injector Test Facility", *Phys. Rev. Accel. Beams*, vol. 19, p. 100702, 2016. `doi:10.1103/PhysRevAccelBeams.19.100702`

[17] F. Marcellini, B. Keil, M. Rohrer, M. Stadler, J. Stettler, D.M. Treyer, D. Lipka, D. Noelle, M. Pelzer, and S. Vilcins, "Design of Cavity BPM Pickups for SwissFEL", in *Proc. IBIC'12*, Tsukuba, Japan, Oct. 2012, paper TUPA24, pp. 390–393. `https://jacow.org/IBIC2012/papers/TUPA24.pdf`